

T1 relaxation time of ISMRM/NIST T1 phantom spheres at 7 T

Yi-Fen Yen¹  | Karl F. Stupic² | Michael T. Janicke³ | Douglas N. Greve¹ |
Azma Mareyam¹ | Jason Stockmann¹ | Jonathan R. Polimeni¹ |
Andre van der Kouwe¹ | Kathryn E. Keenan² 

¹Athinoula A. Martinos Center for Biomedical Imaging, Department of Radiology, Massachusetts General Hospital, Harvard Medical School, Boston, Massachusetts, USA

²Physical Measurement Laboratory, National Institute of Standards and Technology, Boulder, Colorado, USA

³Chemistry Division, Los Alamos National Laboratory, REFOCUS: Resonance Center for Chemical Signatures, Los Alamos, New Mexico, USA

Correspondence

Yi-Fen Yen, Athinoula A. Martinos Center for Biomedical Imaging, Massachusetts General Hospital, Building 149, 13th Street, Room 2303A, Charlestown, MA 02129, USA.
Email: yfen1@mgh.harvard.edu

Funding information

This study was supported by National Institute of Standards and Technology, NIH P41EB015896, R01EB019437, R21AG046657, R01HD071664, R01HD085813, R01HD093578, R01HD099846, R01EB023281, R21AG067562, and R21GM137227. The experiment was made possible by National Institutes of Health NCR Shared Instrumentation Grants S10RR023401 and S10RR020948.

T1 relaxation times of the 14 T1 phantom spheres that make up the standard International Society for Magnetic Resonance in Medicine (ISMRM)/National Institute of Standards and Technology (NIST) system phantom are reported at 7 T. T1 values of six of the 14 T1 spheres at 7 T (with T1 > 270 ms) have been reported previously, but, to the best of our knowledge, not all of the T1s of the 14 T1 spheres at 7 T have been reported before. Given the increasing number of 7-T MRI systems in clinical settings and the increasing need for T1 phantoms that cover a wide range of T1 relaxation times to evaluate rapid T1 mapping techniques at 7 T, it is of high interest to obtain accurate T1 values for all the ISMRM/NIST T1 spheres at 7 T. In this work, T1 relaxation time was measured on a 7-T MRI scanner using an inversion-recovery spin-echo pulse sequence and derived by curve fitting to a signal equation that exhibits insensitivity to B₁⁺ inhomogeneity. Day-to-day reproducibility was within 0.4% and differences between two different RF coils within 1.5%. T1s of a subset of the 14 spheres were also measured by NMR at 7 T for comparison, and the T1 results were consistent between the MRI and NMR measurements. T1 measurements performed at 3 T on the same 14 spheres using the same sequence and fitting method yielded good agreement (mean percentage difference of -0.4%) with the reference T1 values available from the NIST, reflecting the accuracy of the reported technique despite being without the standard phantom housing. We found that the T1 values of all 14 NiCl₂ spheres are consistently lower at 7 T than at 3 T. Although our results were well reproduced, this study represents initial work to quantify the 7-T T1 values of all 14 NIST T1 spheres outside of the standard housing and does not warrant reproducibility of the ISMRM/NIST system phantom as a whole. A future study to assess the T1 values of a version of the ISMRM/NIST system phantom that fits inside typical commercial coils at 7 T will be very helpful. Nonetheless, the details on our acquisition and curve-fitting methods reported here allow the T1 measurements to be reproduced elsewhere. The T1 values of all 14 spheres reported here will be valuable for the development of quantitative MR fingerprinting and rapid T1 mapping

Abbreviations used: 8-ch, eight-channel; 31-ch, 31-channel; CI, confidence interval; FA, flip angle; IR-SE, inversion recovery with spin-echo; ISMRM, International Society for Magnetic Resonance in Medicine; LANL, Los Alamos National Laboratory; MRI, magnetic resonance imaging; NIST, National Institute of Standards and Technology; NMR, nuclear magnetic resonance; RF, radio frequency; ROI, region of interest; SD, standard deviation; TE, echo time; TI, inversion time; TR, repetition time.

The senior authors Andre van der Kouwe and Kathryn E. Keenan contributed equally.

for a large variety of research projects, not only in neuroimaging but also in body MRI, musculoskeletal MRI, and gadolinium contrast-enhanced MRI, each of which is concerned with much shortened T1.

KEYWORDS

3 T, 7 T; NIST phantom, quantitative T1; reproducibility; T1 relaxation time; T1 standard phantom

1 | INTRODUCTION

Quantitative T1 maps are important in many applications, such as deriving quantitative cerebral blood flow from arterial spin labeling MRI data, deriving the volume transfer constant (also known as Ktrans) for blood-brain barrier permeability assessment from dynamic contrast-enhanced MRI data, as well as cortical parcellation for precise morphometry. The International Society for Magnetic Resonance in Medicine (ISMRM) and the National Institute of Standards and Technology (NIST) developed a calibration phantom,^{1,2} consisting of 14 spheres filled with nickel chloride (NiCl₂) solutions of various concentrations, that has been used to validate T1 mapping techniques, as well as for reproducibility comparisons across platforms and sites. The T1 relaxation times of the 14 T1 spheres carefully measured by NMR are available from the NIST to serve as reference or ground truth T1 values at a range of temperatures for 1.5 and 3 T.² The ISMRM/NIST system phantom has thus demonstrated its utility in a large body of research at 1.5 and 3 T for the validation of quantitative methods and assessment of multivendor and multisite repeatability (see^{1,3-16} and the references therein). However, the reference T1 values at 7 T are not available from the NIST. The 7-T T1 values of a subset of the 14 spheres (with T1 > 270 ms) have been reported using three MRI methods¹⁷; precision and reliability were assessed for the subset, but not for all 14 spheres. Given the increasing number of 7-T MRI systems in clinical settings and the growing need for T1 phantoms that cover a wide range of T1 relaxation times to evaluate rapid T1-mapping techniques at 7 T, it is of high interest to obtain accurate T1 values of all 14 spheres at 7 T.

T1 relaxation times of the 14 NiCl₂ spheres from the NIST were measured on a 7-T MRI scanner using an inversion-recovery spin-echo pulse sequence. Day-to-day reproducibility and repeatability using two different RF coils were assessed. The sensitivity of the reported technique to B₁⁺ was evaluated. T1s of a subset of the NiCl₂ spheres were also measured using NMR to evaluate the consistency between the MRI and NMR measurements at 7 T.

The 14 NiCl₂ spheres were used in this study instead of the whole ISMRM/NIST system phantom because the whole phantom was too large to fit inside our custom-made 7-T RF coils. Thus, the 7-T T1 values reported here were assessed in the 14 spheres outside of the standard housing and do not warrant reproducibility to the ISMRM/NIST system phantom as a whole. To further validate our MRI T1 measurement method in the 14 spheres without the standard housing, we measured T1s of the same 14 spheres in the same configuration on a 3-T MRI scanner using the same sequence and curve-fitting method to compare the measured T1s with the NMR reference T1 values at 3 T available from the NIST.

2 | EXPERIMENTAL

2.1 | 7-T MRI experiment

The 14 polycarbonate spheres of 2-cm diameter, filled with NiCl₂ solution of various concentrations, were provided by the NIST to accommodate the small coil geometry in this study. These spheres were spaced 0.4 cm apart, mounted on a rectangular board (Figure 1), and imaged in air (i.e., there was no surrounding fluid). The in-plane area of the NiCl₂ sphere array was 8.8 cm × 10 cm.

T1 mapping experiments were performed on a 7-T Siemens MAGNETOM system (Siemens Healthineers, Erlangen, Germany) using two head coil sets: a 31-channel (31-ch) coil set and an eight-channel (8-ch) coil set, both custom-made at the Martinos Center. The 31-ch coil set consisted of a 31-ch receive loop-array nested within a quadrature birdcage volume coil. The receive array helmet was sized to accommodate a majority of adult heads and was large enough to fit the assembly of only the 14 spheres without standard housing. The receive array had 15 overlapped elements on the top half (with an opening diameter of 8.5 cm) and 16 overlapped elements on the bottom half (with an opening diameter of 9.5 cm). The transmit coil was a de-tunable shielded 16-rung band-pass birdcage with a rung length of 24 cm and rung diameter of 33.5 cm.

The 8-ch coil set comprised a receive array of eight overlapped rectangular elements (6.5 cm × 13 cm) nested inside a quadrature birdcage volume coil. The receive coils were built on eight panels arranged in a U-shape closely around the head (or phantom) to provide a high filling factor

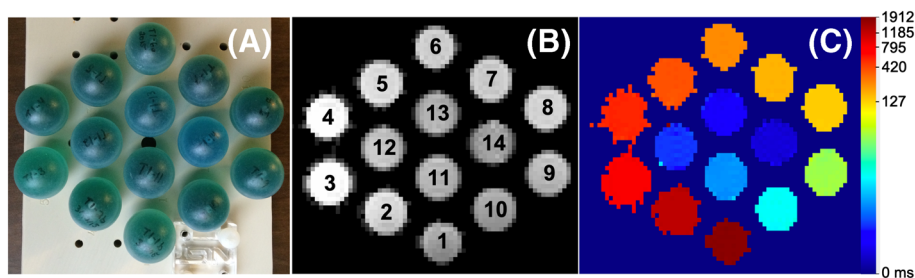


FIGURE 1 (a) Array of 14 NiCl_2 T1 spheres from the NIST used in this work; (b) MR image of the 14 NiCl_2 spheres; and (c) IR-SE T1 map at 7 T. IR-SE, inversion recovery with spin-echo; MR, magnetic resonance; NIST, National Institute of Standards and Technology

and maximal signal-to-noise ratio. The 8-ch coil was too short to wrap around the standard ISMRM/NIST system phantom, but adequate to wrap around the assembly of 14 spheres without the standard housing. The transmit coil was a birdcage similar to the transmit coil used in the 31-ch coil set, except with longer rungs (28 cm) and a smaller diameter (rungs at 30.5 cm and shield at 35.6 cm).

High-order B_0 shimming was performed within a rectangular region of interest (ROI) box just large enough to surround the spheres. The B_1^+ reference voltage was calibrated using the actual flip angle (FA) imaging technique,^{18,19} yielding a map of estimated transmit voltage for a 180° reference pulse (hard pulse of 1-ms pulse width). The mean voltage was then entered manually as the reference voltage for the remaining acquisitions performed within the same imaging session.

We used an inversion recovery with spin-echo (IR-SE) sequence from the vendor (Siemens Healthineers) to measure T1 relaxation times of the T1 spheres at 7 T. The IR-SE sequence employed a 10.24-ms hyperbolic secant RF pulse^{20,21} to produce nonslice-selective adiabatic inversion to minimize the sensitivity to B_1^+ variations. K-space data were acquired in five segments from five spin-echoes (a turbo factor of 5). The 90° excitation and 180° refocusing RF pulses were amplitude-modulated sinc pulses of 1.024- and 1.28-ms durations, respectively. The IR-SE imaging parameters are as follows: TR/TE/FA = 12.5 s/6.4 ms/ 90° , 0.16 cm x 0.16 cm, a single 0.6-cm coronal slice, receiver bandwidth of 300 Hz/pixel, and TIs of 24, 50, 75, 100, 125, 150, 250, 500, 750, 1000, 2000, and 3000 ms. The whole series took 70 min. A very long TR was chosen to ensure full T1 recoveries of all 14 samples and also to eliminate sensitivities to the FA of the excitation RF pulse. To assess the sensitivity of IR-SE to B_1^+ , we purposely offset the reference voltage of the 1-ms rectangular reference pulse by $\pm 20\%$ from the optimal reference voltage to compare resulting T1 measurements from the phantom. This reference voltage offset affected all RF pulses, although the adiabatic pulses were in principle less sensitive to the change. In addition, reproducibility of the IR-SE acquisitions was assessed between the two different coil sets. The 31-ch coil set was also used to measure test and retest reproducibility on two separate days.

2.2 | 7-T NMR experiment

To validate our T1 measurements performed on a clinical MRI scanner with NMR measurements, we collaborated with Los Alamos National Laboratory (LANL), where a 300-MHz Bruker AVANCE spectrometer (Billerica, MA, USA) was available. The T1 relaxation times of a subset of the NiCl_2 array were measured using IR pulse sequences at 7 T using standard 0.5-cm NMR sample tubes as received from the NIST. These flame-sealed reference samples maintained by the NIST were full NMR tubes, each with a different concentration of NiCl_2 solution. The data collected suffered from radiation dampening. Because the solvent (water) was the only proton of observation, we could not employ the typical solvent suppression NMR pulse sequences to reduce radiation dampening. We chose to move the resonant frequency of the NMR probe (i.e., to detune) to reduce the radiation-dampening effect, while accepting a reduction in signal-to-noise. A conventional IR pulse sequence was used to acquire the relaxation data. The decay curves were analyzed with MNova software available from Mestrelab (Santiago de Compostela, Spain).

2.3 | 3-T MRI experiment

Because we were concerned about the effect of measuring these spheres without the standard phantom housing, we also measured T1 relaxation times of the 14 T1 spheres in air using the same IR-SE sequence at 3 T, at which field strength the NMR reference T1 values are available from the NIST.^{1,22} Our T1 measurements at 3 T were performed on a 3-T Siemens Prisma MRI system using a 32-ch head coil from the manufacturer. We used the same IR-SE imaging parameters as those used to collect the 7-T data.

2.4 | Data analysis

T1 maps were generated by fitting the series of magnitude images with variable TIs using the following equation²³:

$$S(TI) = |a + b e^{-TI/T1}|, \quad (1)$$

where $S(TI)$ is the magnitude signal at the time of inversion (TI). The interpretation of the fitting parameters a and b are described in detail in.²³ This method does not require perfect inversion pulses, and the fitting speed is largely improved by using a reduced-dimension nonlinear least squares algorithm.²³ Matlab (Natick, MA, USA) code is available at <http://www-mrsrl.stanford.edu/~jbarra/t1map.html> and <https://github.com/qMRLab/qMRLab>. After obtaining the T1 maps, ROI analyses were performed on the T1 maps with circles of 1.4-cm diameter (which comprised approximately 60 pixels) manually placed in the center of each sphere on the T1 maps, to calculate the mean and standard deviation of T1 values of each sphere.

To quantify reproducibility tests, we used the Bland–Altman analysis method described in.^{24,25} For each pair of measurements in a comparison (either repeated measurements on two different days, or measurements by using two different coils, or with different B_1^+ offsets, or agreement between MRI and NMR measurements), the percentage difference was calculated as $100 \times (\text{measurement A} - \text{measurement B}) / (\text{mean of measurement A and measurement B})$ for each sphere. The mean percentage difference of all 14 spheres was used to quantify the degree of agreement between the measurements. The limits of agreement, which give a range within which we expect 95% of future differences in measurements to occur, were calculated as $(\text{mean percentage difference} \pm 1.96 \times \text{SD})$, where SD is the standard deviation of the percentage differences of all 14 spheres. The limits of agreement are estimates. We then calculated the 95% confidence interval (CI) of the upper limit as $(\text{upper limit} \pm 1.96 \times 1.71 \times \text{SD} / \sqrt{n})$ and the 95% CI of the lower limit as $(\text{lower limit} \pm 1.96 \times 1.71 \times \text{SD} / \sqrt{n})$, where $n = 14$.

3 | RESULTS

3.1 | 7-T MRI experiment

Figure 1 shows the array of 14 T1 spheres, the MR image of the spheres, and the IR-SE T1 map acquired at 7 T. The NiCl_2 concentration of each of the 14 spheres, their mean and SD T1 obtained at Massachusetts General Hospital (MGH) at 7 and 3 T, as well as the 7-T NMR T1 values from

TABLE 1 NiCl_2 concentrations of the 14 spheres that made up the ISMRM/NIST system phantom; their mean T1 relaxation times and T1 SDs are also listed. The MGH MRI T1 values were measured from the 14 T1 spheres in air at 7 T and at 3 T. The LANL NMR T1 values were measured on a subset of the NiCl_2 solutions. The NIST NMR T1 values at 3 T were provided by the NIST from prior work

Sample name	[NiCl_2] (mM)	7 T				3 T			
		MGH MRI T1 (ms)	MGH MRI SD (ms)	LANL NMR T1 (ms)	LANL NMR SD (ms)	MGH MRI T1 (ms)	MGH MRI SD (ms)	NIST NMR T1 (ms)	NIST NMR SD (ms)
T1-1	0.299	1804	39			1927	32	1989	1
T1-2	0.623	1252	13			1425	15	1454	3
T1-3	1.072	811	13	837	42	974.0	5.8	984.1	0.3
T1-4	1.720	563	14			696.7	4.1	706.0	1.5
T1-5	2.617	398.5	4.0	395	20	497.0	2.7	496.7	0.4
T1-6	3.912	279.9	1.4			353.5	1.7	351.5	0.9
T1-7	5.731	194.9	1.3	197.0	9.9	248.8	1.0	247.1	0.1
T1-8	8.297	137.9	1.0			177.5	0.9	175.3	0.1
T1-9	11.94	97.3	1.1	97.4	4.9	125.6	0.7	125.9	0.3
T1-10	17.07	68.3	1.1			88.4	0.5	89.00	0.17
T1-11	24.33	48.2	0.8	47.3	2.4	62.7	0.4	62.70	0.13
T1-12	34.59	33.8	1.0			44.5	0.5	44.53	0.09
T1-13	49.12	23.1	2.7			31.2	0.5	30.84	0.02
T1-14	69.68	15.0	3.2			21.4	1.2	21.72	0.01

Abbreviations: ISMRM, International Society for Magnetic Resonance in Medicine; LANL, Los Alamos National Laboratory; MGH, Massachusetts General Hospital (MGH); MRI, magnetic resonance imaging; NIST, National Institute of Standards and Technology; SD, standard deviation.

LANL and 3-T NMR reference T1 values provided by the NIST, are listed in Table 1. Examples of curve-fitting results are shown in Figure 2 to demonstrate the quality of the fit. Each curve was an MR signal time curve of a single pixel randomly picked from a sphere, as identified by the sphere ID in Figure 2. Curve-fitting error averaged over the ROI of each sphere ranged from 0.4% to 1.8%. The SD of each T1 sphere from each

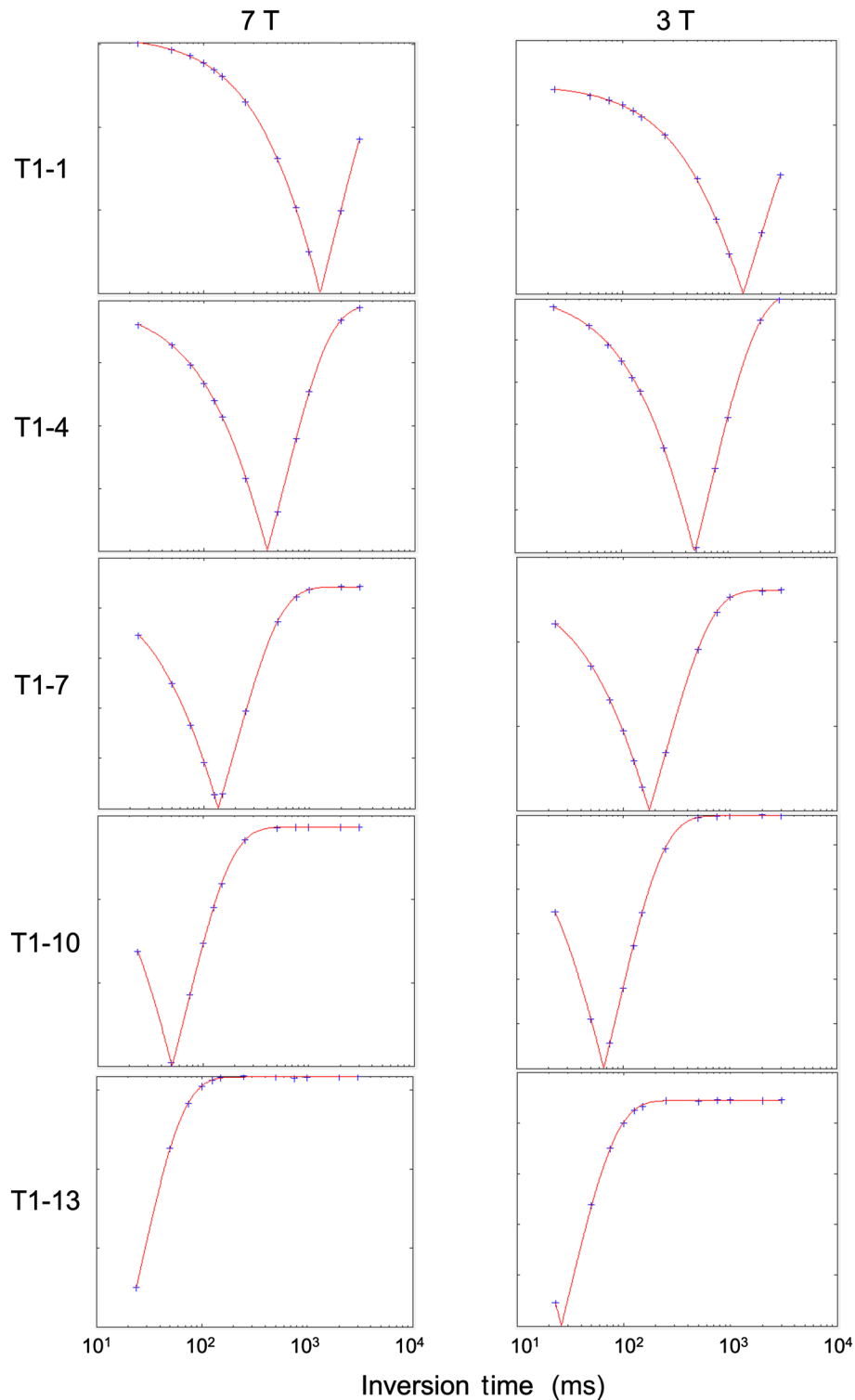


FIGURE 2 Exemplified T1 curve-fitting results. Each curve was an MR signal time curve of a single pixel randomly picked from a sphere, as identified by the sphere ID. Blue crosses are the MRI data and red curves are the fit. The y-axis is the MRI signal (arbitrary units) and the X-axis is the inversion time (ms). MR, magnetic resonance; MRI, magnetic resonance imaging

IR-SE measurement was the SD of the pixel-wise fitted T1 values within the ROI of each sphere. The reported SD measured on the 7-T MRI scanner at MGH in Table 1 (listed as “MGH MRI SD”) is the root-mean-square of the SD values from all test and retest data (day-to-day with 8- or 31-ch coil) acquired at the optimal B_1^+ reference voltage settings.

The IR-SE T1 measurements at 7 T were reproducible, both when tested on two separate days using the same coil (Figure 3) or when tested using two different coil sets on two different days (Figure 4). Comparing T1 measured on day 2 with day 1, the mean percentage difference was 0.4%; the upper limit of agreement was 5.4% (CI: 4.3% to 6.6%); and the lower limit of agreement was -4.7% (CI: -5.9% to -3.5%). Comparing T1 measured by using the 31-ch coil set with the 8-ch coil set, the mean percentage difference was 1.5%; the upper limit of agreement was 6.5% (CI: 5.3% to 7.7%); and the lower limit of agreement was -3.5% (CI: -4.7% to -2.3%).

At 7 T, the estimated B_1^+ had a spatial variation of approximately $\pm 15\%$ across all the spheres. Among the eight imaging sessions, each conducted on a different day, the optimal B_1^+ reference voltage varied by approximately $\pm 6.5\%$. When we intentionally offset the reference voltage by $\pm 20\%$ from the optimal reference voltage, we found the T1 results did not deviate substantially (Figure 5). Percentage difference between T1 measured at 80% B_1^+ and T1 at 100% B_1^+ (i.e., optimal B_1^+ with no offset) was plotted as a function of \log_2 of the T1 at 100% B_1^+ (Figure 5B); \log_2 of T1 was used in the plot for easy visualization of the low-T1 datapoints. Comparing T1 measured at 80% B_1^+ with T1 at 100% B_1^+ , the mean percentage difference was -2.0% ; the upper limit of agreement was 4.1% (CI: 2.7% to 5.6%); and the lower limit of agreement was -8.0% (CI: -9.5% to -6.6%). Comparing T1 measured at 120% B_1^+ with T1 at 100% B_1^+ (Figure 5C), the mean percentage difference was 0.4%; the upper limit of agreement was 4.3% (CI: 3.4% to 5.2%); and the lower limit of agreement was -3.5% (CI: -4.4% to -2.6%).

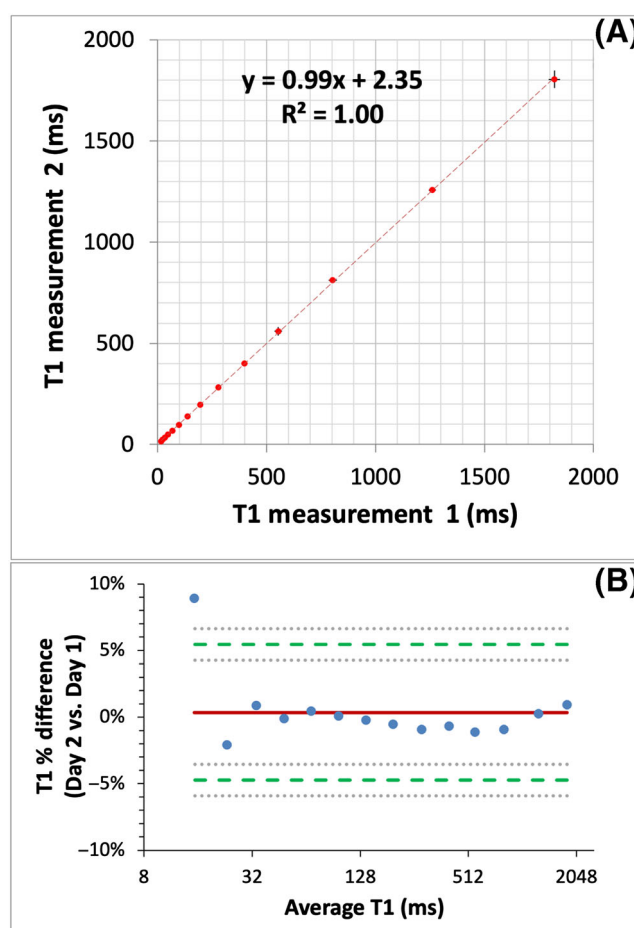


FIGURE 3 Reproducibility of the IR-SE T1 measurements at 7 T. (A) The T1 values measured on day 2 versus those measured on day 1, using the same coil (31-ch coil set). (B) The Bland–Altman plot shows the percentage difference between the T1 measured on day 2 versus T1 on day 1 against the average T1 measured on the two days. The red solid line indicates the mean percentage difference; the upper green dashed line shows mean + 1.96 SD (upper limit of agreement) and the lower green dashed line shows mean $- 1.96$ SD (lower limit of agreement), each with 95% confidence intervals (gray dotted lines). 31-ch, 31-channel; IR-SE, inversion recovery with spin-echo; SD, standard deviation

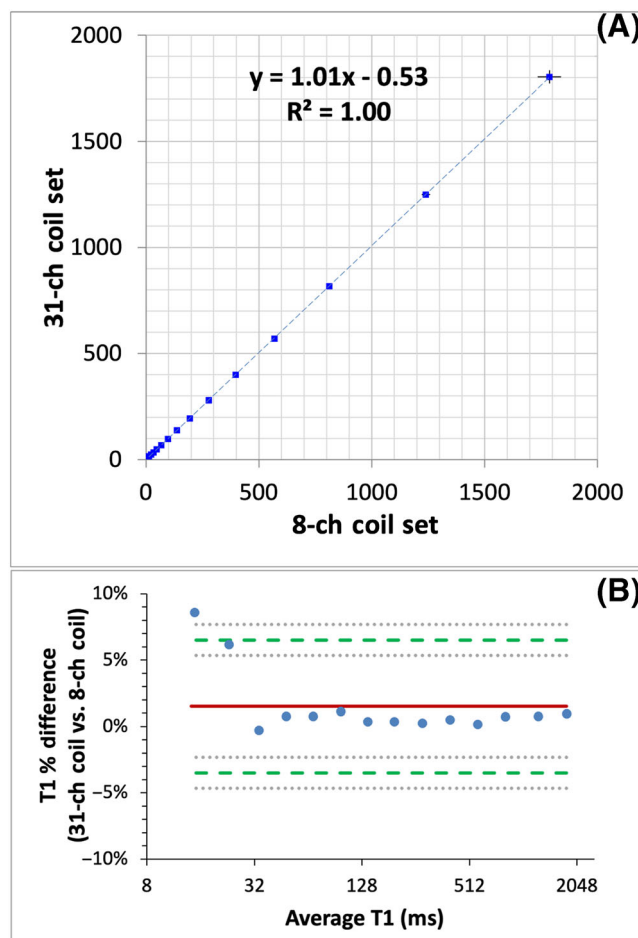


FIGURE 4 Reproducibility of the IR-SE T1 measurements at 7 T. (A) The T1 measurements using the 31-ch coil set versus those using the 8-ch coil set. (B) The Bland-Altman plot shows the percentage difference between the T1 measured by the 31-ch coil set versus T1 measured by the 8-ch coil set against the average T1 by the two coil sets. The red solid line indicates the mean percentage difference; the upper green dashed line shows mean + 1.96 SD (upper limit of agreement) and the lower green dashed line shows mean - 1.96 SD (lower limit of agreement), each with 95% confidence intervals (gray dotted lines). 8-ch, eight-channel; 31-ch, 31-channel; IR-SE, inversion recovery with spin-echo; SD, standard deviation

3.2 | 3-T MRI experiment

We found good agreement between our 3-T T1 measurements of the spheres without standard phantom housing versus the ground truth T1 values at 3 T provided by the NIST (Figure 6B). The mean percentage difference was -0.4%; the upper limit of agreement was 2.0% (CI: 1.4% to 2.6%); and the lower limit of agreement was -2.9% (CI: -3.4% to -2.3%).

3.3 | 7-T NMR experiment

Good agreement was also achieved between our 7-T T1 measurements using clinical MRI scanners versus the NMR T1 measurements at 7 T (Figure 6A). The mean percentage difference was -0.3%; the upper limit of agreement was 3.5% (CI: 2.0% to 4.9%); and the lower limit of agreement was -4.1% (CI: -5.6% to -2.6%). Because of the restrictions presented by the 7-T NMR instrument used for these data, the SD reported here (Table 1: LANL NMR SD) is larger than that for the previously reported NMR data from the NIST at 1.5 and 3 T (Table 1: NIST NMR SD). The SD of the LANL 7-T NMR T1 accounts for system differences, including less accurate temperature measurements, different sample geometry, pulse sequence difference, and system homogeneity. For example, the temperature control on the 7-T NMR was estimated to be $\pm 1^\circ\text{C}$ compared with 1.5- and 3-T NMR measurements at $\pm 0.25^\circ\text{C}$, thus increasing the SD.

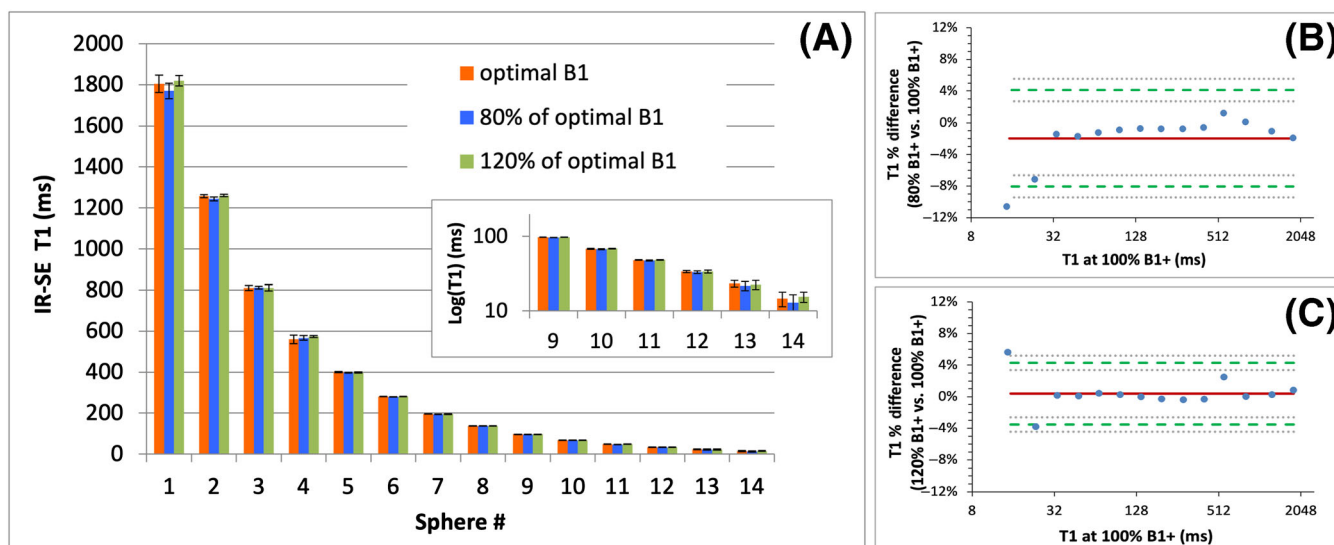


FIGURE 5 The IR-SE T1 measurement is insensitive to B_1^+ variations within $\pm 20\%$ offset from the optimal B_1^+ reference voltage. (A) The mean and SD of T1 from each sphere ROI at each B_1^+ reference voltage performed within the same imaging session. (B) The Bland-Altman plot shows the percentage difference between the T1 measured at 80% B_1^+ versus T1 measured at 100% B_1^+ (i.e., optimal B_1^+ of that imaging session) against the T1 at 100% B_1^+ . (C) The Bland-Altman plot shows the percentage difference between the T1 measured at 120% B_1^+ versus T1 measured at 100% B_1^+ against the average T1 at 100% B_1^+ . The red solid line indicates the mean percentage difference; the upper green dashed line shows mean + 1.96 SD (upper limit of agreement) and the lower green dashed line shows mean - 1.96 SD (lower limit of agreement), each with 95% confidence intervals (gray dotted lines). IR-SE, inversion recovery with spin-echo; ROI, region of interest; SD, standard deviation

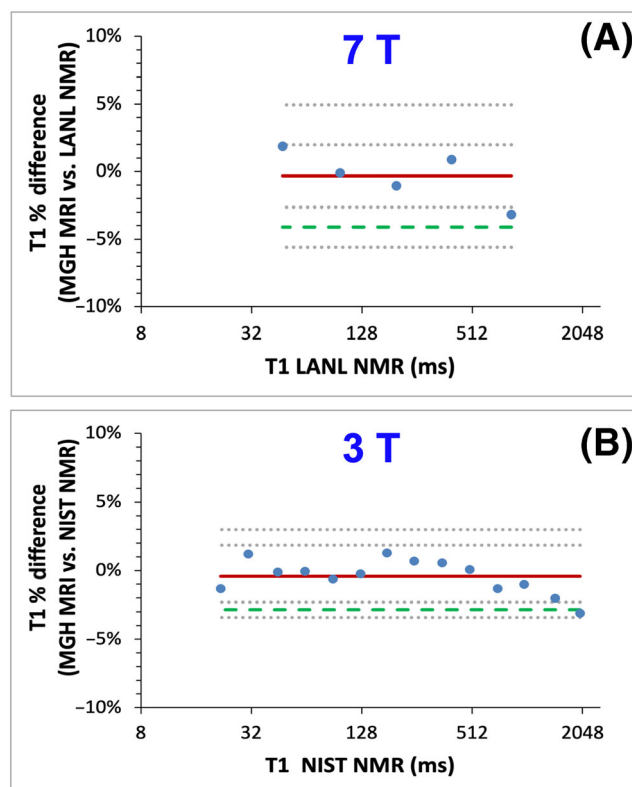


FIGURE 6 Agreement between the IR-SE T1 measurements using clinical MRI scanners versus NMR T1 measurements on the same NiCl_2 solutions from the NIST at (A) 7 T and (B) 3 T. Percentage differences of T1 are plotted against the T1 measured by NMR. The red solid line indicates the mean percentage difference; the upper green dashed line shows mean + 1.96 SD (upper limit of agreement) and the lower green dashed line shows mean - 1.96 SD (lower limit of agreement), each with 95% confidence intervals (gray dotted lines). IR-SE, inversion recovery with spin-echo; LANL, Los Alamos National Laboratory; MGH, Massachusetts General Hospital; MRI, magnetic resonance imaging; NIST, National Institute of Standards and Technology; NMR, nuclear magnetic resonance; SD, standard deviation

4 | DISCUSSION

We report T1 measurements of the 14 T1 spheres, which make up the standard ISMRM/NIST system phantom, at 7 and 3 T. Ideally, phantom imaging should be performed with fluid surrounding the objects of interest to eliminate susceptibility signal loss and to produce better shim for homogeneous B₀. Because both of our custom-made RF coils at 7 T were too small to accommodate the standard ISMRM/NIST system phantom, we obtained the 14 NiCl₂ T1 spheres from the NIST and imaged them in air. To evaluate the potential errors because of this nonideal experimental setup, we performed a similar experiment at 3 T on the same phantom. The resulting T1 values were in agreement with (within 3% of) the reference standards from the NIST. T1 values at 7 T were reproduced within a narrow margin, comparing measurements performed on two separate days or those on two different coil sets.

We noticed that the sphere with the lowest T1 (15 ms) at 7 T tends to have the greatest percentage differences in the reproducibility tests, as shown in the Bland–Altman plots in Figures 3, 4, and 5B. This may be attributable to the lowest inversion time (24 ms) acquired not being low enough for a precise T1 measurement of the sphere with 15-ms T1. In addition, for such a short T1, relaxation during the RF pulse may also contribute to measurement error.

Another potential limitation is the B₁⁺ inhomogeneity at 7 T. The spatial variation of B₁⁺ observed by us was probably comparable with that observed by Sanchez Panchuelo et al.¹⁷ They showed a B₁⁺ variation of 40% between the sphere of the highest B₁⁺ (~85%) and the sphere of the lowest B₁⁺ (~45%) (see supplementary material fig. 3A in¹⁷) inside their 16-cm diameter phantom housing, which was modified to fit their 7-T NOVA coil. From their figure, the longest distance between spheres is approximately 12 cm. We used the actual FA imaging technique to estimate the transmit reference voltage and found a spatial variation of approximately ± 15% (i.e., a 30% span) across all the spheres over an area of 8.8 cm × 10 cm. Although we have shown that our T1 estimation method was relatively robust within ± 20% of the optimal B₁⁺ reference voltage, a better method would have been to incorporate B₁⁺ correction in the data analysis prior to curve fitting to estimate T1.

It is worth mentioning that the curve-fitting method used here takes into account nonideal inversion pulses and makes a noticeable difference to the T1 results, especially at high field. For example, we first reported preliminary T1 values of the 14 T1 spheres at 7 and 3 T at the ISMRM annual meeting in 2017²⁶ by using the signal equation of the IR sequence assuming ideal inversion pulses. The limit of agreement (defined as mean percentage difference ± 1.96 × SD; see the Experimental section) between our 2017 T1 values at 3 T and the reference T1s from the NIST was −1.6% ± 3.1%. With the same data but using the curve-fitting method reported here, we obtained a better agreement between our T1 values at 3 T and the NIST reference T1s (limit of agreement = −0.4% ± 2.4%). At 7 T, where B₁⁺ inhomogeneity is even more severe than at 3 T, we found a substantial discrepancy between our 7-T T1 values assuming ideal inversion pulses²⁶ versus the T1s reported here (limit of agreement = 3.4% ± 6.3%).

Sanchez Panchuelo et al.¹⁷ reported T1 relaxation times for six of the 14 spheres (T1-1 to T1-6) using three rapid T1-mapping methods at 7 T: IR-echo planar imaging (EPI), multislice IR EPI (MS-IR-EPI), and Magnetization-Prepared 2 Rapid Gradient Echoes (MP2RAGE) on the standard ISMRM/NIST system phantom. They did not report T1 values using the IR-SE method at 7 T. Their reported T1 of sphere T1-6 was 406 ± 7 ms, which may be a typographical error as the value is larger than their T1 value of a less concentrated sphere (T1-5 T1 = 388 ± 2 ms), when the reverse is expected. When excluding the T1-6 data, the limit of agreement between their T1 values measured by IR-EPI and ours measured by IR-SE at 7 T is −2.4% ± 5.4%, which is noticeably different.

While it is difficult to judge which 7-T measurements are more accurate (reference 7-T T1 values are unavailable from the NIST), we can compare our 3-T IR-SE T1 measurements with those from Sanchez Panchuelo et al. for spheres T1-1 to T1-6 that were also reported in¹⁷ using the standard ISMRM/NIST system phantom. The limit of agreement between their IR-SE T1 values at 3 T and the NIST reference T1 values is −0.8% ± 5.6%. We obtained slightly better agreement between our 3-T T1 values (from the array of 14 T1 spheres) and the NIST reference T1s (limit of agreement = −0.4% ± 2.4%), which suggests that our method yielded slightly more accurate and more precise T1 results than those obtained using their method, which may have been selected for practical acquisition times rather than optimal accuracy and precision. Contributing factors may be the longer TR (12.5 s) used in our IR-SE measurements compared with theirs (5 s) and the curve-fitting method, which takes into account nonideal inversion pulses. The latter is even more critical at 7 than at 3 T.

T1 relaxation time varies with temperature. In this study, the T1 spheres mounted on a rectangular board were left in the scanner suite, which has temperature-controlled airflow at approximately 20°C, at least overnight before each imaging session to reach temperature equilibrium. Temperature of the spheres was measured in some imaging sessions but not every session with an infrared thermometer of unknown accuracy. This may pose limitations to the accuracy of our T1 measurements. According to Stupic et al.,² over a range of 18 to 22°C, the T1s of NiCl₂ solutions vary by ± 3% relative to the T1s at 20°C.

It has been reported that the NiCl₂ solutions used in the ISMRM/NIST system phantom have lower T1 relaxation times at 3 T than those at 1.5 T.^{1,22} We found a similar trend with lower T1s at 7 T than at 3 T. T1 of NiCl₂ has complex temperature and B₀ field strength dependency, as previously described.^{27,28} The B₀ field dependency of T1 for these 14 particular NiCl₂ spheres has been reported by Stupic et al.² For readers interested in the exact field strengths at which our work was conducted, our “7 T” data were acquired at 6.980 T and our “3 T” data were acquired at 2.893 T. The LANL “7 T” NMR data were acquired at 7.049 T (operating ¹H frequency for the NMR spectrometer = 300.13 MHz). The NIST “3 T” NMR measurements quoted in^{1,22} were acquired at 3.00 T.

Although our results reproduced well, this study represents initial work to quantify the 7-T T₁ values of all 14 T₁ spheres outside of the standard housing and does not warrant reproducibility to the ISMRM/NIST system phantom as a whole. The T₁ measurements at 7 T may be further improved in the future by mapping each individual sphere one at a time with surrounding fluid or designing a smaller standard phantom that fits in coils available at most 7-T scanners. The ubiquitous Nova head coil (Nova Medical, Wilmington, DE, USA), for example, has dimensions of approximately 18.4 cm (width) × 21.6 cm (height) × 20.3 cm (depth). The standard ISMRM/NIST system phantom does not fit inside the Nova coil. The Essential System Phantom (CaliberMRI, Boulder, CO, USA) is smaller than the ISMRM/NIST system phantom, but is still too large to fit inside the Nova coil. The MultiSample120S cylindrical phantom (Gold Standard Phantoms, Rochester, UK) would probably fit inside the Nova coil, but is limited to eight 15-ml polypropylene centrifuge tubes. In addition to the concern with phantom size, dielectric resonance effects increase with field strength, and as the transmit wavelength approaches the size of the head, interference patterns cause inhomogeneous transmit efficiency at 7 T. It is most likely that the existing NIST phantoms are not sufficient, and the 7-T community would benefit from a new standard phantom that incorporates both known relaxation properties and appropriate electromagnetic properties^{29–31} for pulse sequence testing.

In conclusion, we reported the T₁ relaxation times of the 14 NiCl₂ T₁ spheres from the NIST at 7 T using the IR-SE technique. We showed the robustness of IR-SE within ± 20% B₁⁺ variations. IR-SE T₁ measurements were reproduced on two separate days and on two different coil sets. Even although T₁ values were obtained by imaging the 14 T₁ spheres in air on a clinical MRI scanner, our 3-T T₁ values are in good agreement with the reference T₁ values from the NIST and a subset of our 7-T T₁ values are in good agreement with the NMR T₁ values from LANL. A new standard system phantom that fits inside most commercial coils at 7 T and has appropriate electromagnetic properties would be beneficial to the 7-T community. Nonetheless, the details of our acquisition and curve-fitting methods reported here allow the T₁ measurements to be reproduced elsewhere. The T₁ values of all 14 spheres reported here will be valuable for the development of quantitative MR fingerprinting and rapid T₁ mapping for a large variety of research projects, not only in neuroimaging, but also in body MRI, musculoskeletal MRI, and gadolinium contrast-enhanced MRI, each of which is concerned with much shortened T₁.

ACKNOWLEDGMENTS

This study was supported by National Institute of Standards and Technology, NIH P41EB015896, R01EB019437, R21AG046657, R01HD071664, R01HD085813, R01HD093578, R01HD099846, R01EB023281, R21AG067562, and R21GM137227. The experiment was made possible by National Institutes of Health NCRR Shared Instrumentation Grants S10RR023401 and S10RR020948.

CONFLICT OF INTEREST

All authors disclose no relevant conflicts of interest.

NIST REQUIRED DISCLAIMER

Certain commercial instruments and software are identified to specify the experimental study adequately. This does not imply endorsement by NIST or that the instruments and software are the best available for the purpose.

ORCID

Yi-Fen Yen  <https://orcid.org/0000-0001-9986-5327>

Kathryn E. Keenan  <https://orcid.org/0000-0001-9070-5255>

REFERENCES

- Keenan KE, Stupic KF, Boss MA, et al., eds. In: Multi-site, multi-vendor comparison of T₁ measurement using ISMRM/NIST system phantom: Proc 24th Intl Soc Mag Reson Med #3290. Singapore: Wiley; 2016.
- Stupic KF, Ainslie M, Boss MA, et al. A standard system phantom for magnetic resonance imaging. *Magn Reson Med*. 2021;86(3):1194–1211. doi:10.1002/mrm.28779
- Campbell-Washburn AE, Jiang Y, Korzdorfer G, Nittka M, Griswold MA. Feasibility of MR fingerprinting using a high-performance 0.55 T MRI system. *Magn Reson Imaging*. 2021;81:88–93. doi:10.1016/j.mri.2021.06.002
- Carr ME, Keenan KE, Rai R, Metcalfe P, Walker A, Holloway L. Determining the longitudinal accuracy and reproducibility of T₁ and T₂ in a 3T MRI scanner. *J Appl Clin Med Phys*. 2021;22(11):143–150. doi:10.1002/acm2.13432
- Jiang Y, Ma D, Keenan KE, Stupic KF, Gulani V, Griswold MA. Repeatability of magnetic resonance fingerprinting T₁ and T₂ estimates assessed using the ISMRM/NIST MRI system phantom. *Magn Reson Med*. 2017;78(4):1452–1457. doi:10.1002/mrm.26509
- Kato Y, Ichikawa K, Okudaira K, et al. Comprehensive evaluation of B₁(+)-corrected FISP-based magnetic resonance fingerprinting: accuracy, repeatability and reproducibility of T₁ and T₂ relaxation times for ISMRM/NIST system phantom and volunteers. *Magn Reson Med Sci*. 2020;19(3):168–175. doi:10.2463/mrms.mp.2019-0016
- Keenan KE, Gimbutas Z, Dienstfrey A, et al. Multi-site, multi-platform comparison of MRI T₁ measurement using the system phantom. *PLoS ONE*. 2021;16(6):e0252966. doi:10.1371/journal.pone.0252966
- Ma D, Jones SE, Deshmane A, et al. Development of high-resolution 3D MR fingerprinting for detection and characterization of epileptic lesions. *J Magn Reson Imaging*. 2019;49(5):1333–1346. doi:10.1002/jmri.26319

9. Murata S, Hagiwara A, Fujita S, et al. Effect of hybrid of compressed sensing and parallel imaging on the quantitative values measured by 3D quantitative synthetic MRI: A phantom study. *Magn Reson Imaging*. 2021;78:90-97. doi:[10.1016/j.mri.2021.01.001](https://doi.org/10.1016/j.mri.2021.01.001)
10. Nejad-Davarani SP, Zakariaei N, Chen Y, et al. Rapid multicontrast brain imaging on a 0.35T MR-linac. *Med Phys*. 2020;47(9):4064-4076. doi:[10.1002/mp.14251](https://doi.org/10.1002/mp.14251)
11. Pirastru A, Chen Y, Pelizzari L, et al. Quantitative MRI using STRategically Acquired Gradient Echo (STAGE): optimization for 1.5 T scanners and T1 relaxation map validation. *Eur Radiol*. 2021;31(7):4504-4513. doi:[10.1007/s00330-020-07515-z](https://doi.org/10.1007/s00330-020-07515-z)
12. Sharafi A, Zibetti MVW, Chang G, Cloos MA, Regatte RR. Simultaneous bilateral T1, T2, and T1rho relaxation mapping of the hip joint with magnetic resonance fingerprinting. *NMR Biomed*. 2022;35(5):e4651. doi:[10.1002/nbm.4651](https://doi.org/10.1002/nbm.4651)
13. Shridhar Konar A, Qian E, Geethanath S, et al. Quantitative imaging metrics derived from magnetic resonance fingerprinting using ISMRM/NIST MRI system phantom: An international multicenter repeatability and reproducibility study. *Med Phys*. 2021;48(5):2438-2447. doi:[10.1002/mp.14833](https://doi.org/10.1002/mp.14833)
14. Statton BK, Smith J, Finnegan ME, Koerzdoerfer G, Quest RA, Grech-Sollars M. Temperature dependence, accuracy, and repeatability of T1 and T2 relaxation times for the ISMRM/NIST system phantom measured using MR fingerprinting. *Magn Reson Med*. 2022;87(3):1446-1460. doi:[10.1002/mrm.29065](https://doi.org/10.1002/mrm.29065)
15. Tong G, Gaspar AS, Qian E, et al. A framework for validating open-source pulse sequences. *Magn Reson Imaging*. 2022;87:7-18. doi:[10.1016/j.mri.2021.11.014](https://doi.org/10.1016/j.mri.2021.11.014)
16. Wang Y, Tadimalla S, Rai R, et al. Quantitative MRI: Defining repeatability, reproducibility and accuracy for prostate cancer imaging biomarker development. *Magn Reson Imaging*. 2021;77:169-179. doi:[10.1016/j.mri.2020.12.018](https://doi.org/10.1016/j.mri.2020.12.018)
17. Sanchez Panchuelo RM, Mougín O, Turner R, Francis ST. Quantitative T1 mapping using multi-slice multi-shot inversion recovery EPI. *NeuroImage*. 2021;234:117976. doi:[10.1016/j.neuroimage.2021.117976](https://doi.org/10.1016/j.neuroimage.2021.117976)
18. Hartwig V, Vanello N, Giovannetti G, et al. B(1)(+)/actual flip angle and reception sensitivity mapping methods: simulation and comparison. *Magn Reson Imaging*. 2011;29(5):717-722. doi:[10.1016/j.mri.2011.01.004](https://doi.org/10.1016/j.mri.2011.01.004)
19. Yarnykh VL. Actual flip-angle imaging in the pulsed steady state: a method for rapid three-dimensional mapping of the transmitted radiofrequency field. *Magn Reson Med*. 2007;57(1):192-200. doi:[10.1002/mrm.21120](https://doi.org/10.1002/mrm.21120)
20. Bernstein MA, King KF, Zhou XJ. Chapter 6 - Adiabatic Radiofrequency Pulses. In: *Handbook of MRI Pulse Sequences*. Elsevier Inc; 2004:177-212.
21. Garwood M, Ugurbil K. B1 Insensitive Adiabatic RF Pulses. In: Rudin M, ed. *In-Vivo Magnetic Resonance Spectroscopy I: Probeheads and Radiofrequency Pulses Spectrum Analysis*. Springer; 1992.
22. Bane O, Hectors SJ, Wagner M, et al. Accuracy, repeatability, and interplatform reproducibility of T1 quantification methods used for DCE-MRI: Results from a multicenter phantom study. *Magn Reson Med*. 2018;79(5):2564-2575. doi:[10.1002/mrm.26903](https://doi.org/10.1002/mrm.26903)
23. Barral JK, Gudmundson E, Stikov N, Etezadi-Amoli M, Stoica P, Nishimura DG. A robust methodology for in vivo T1 mapping. *Magn Reson Med*. 2010;64(4):1057-1067. doi:[10.1002/mrm.22497](https://doi.org/10.1002/mrm.22497)
24. Bartlett JW, Frost C. Reliability, repeatability and reproducibility: analysis of measurement errors in continuous variables. *Ultrasound Obstet Gynecol*. 2008;31(4):466-475. doi:[10.1002/uog.5256](https://doi.org/10.1002/uog.5256)
25. Giavarina D. Understanding Bland Altman analysis. *Biochem Med*. 2015;25(2):141-151. doi:[10.11613/BM.2015.015](https://doi.org/10.11613/BM.2015.015)
26. Yen YF, Keenan KE, Stupic KF, Van der Kouwe A, Polimeni JR. T1 Mapping of NIST Phantom at 7T. *Proc 25th Intl Soc Mag Reson Med #5207*. Honolulu, USA: Wiley; 2017.
27. Kowalewski J, Egorov A, Kruk D, et al. Extensive NMRD studies of Ni (II) salt solutions in water and water-glycerol mixtures. *J Magn Reson*. 2008;195(1):103-111. doi:[10.1016/j.jmr.2008.08.011](https://doi.org/10.1016/j.jmr.2008.08.011)
28. Kraft KA, Fatouros PP, Clarke GD, Kishore PR. An MRI phantom material for quantitative relaxometry. *Magn Reson Med*. 1987;5(6):555-562. doi:[10.1002/mrm.1910050606](https://doi.org/10.1002/mrm.1910050606)
29. *Dielectric Phantom Recipe Generator: by Advanced MRI*. NIH: NINDS; 2016. Accessed December 9, 2016. <https://amri.ninds.nih.gov/cgi-bin/phantomrecipe>
30. Phantom Recipe Generator: An Online Calculator for Creating Dielectric MRI Phantoms.: by Center for Advanced Imaging Innovation and Research; 2022. Accessed January 1, 2014. <https://cai2r.net/resources/phantom-recipe-generator/>
31. Ianniello C, de Zwart JA, Duan Q, et al. Synthesized tissue-equivalent dielectric phantoms using salt and polyvinylpyrrolidone solutions. *Magn Reson Med*. 2018;80(1):413-419. doi:[10.1002/mrm.27005](https://doi.org/10.1002/mrm.27005)

How to cite this article: Yen Y-F, Stupic KF, Janicke MT, et al. T1 relaxation time of ISMRM/NIST T1 phantom spheres at 7 T. *NMR in Biomedicine*. 2023;36(5):e4873. doi:[10.1002/nbm.4873](https://doi.org/10.1002/nbm.4873)